AFRL-RX-WP-JA-2016-0251

COMPOSITIONAL CONTROL OF THE MIXED ANION ALLOYS IN GALLIUM-FREE InAs/InAsSb SUPERLATTICE MATERIALS FOR INFRARED SENSING (POSTPRINT)

H. J. Haugan, F. Szmulowicz, K. Mahalingam, G. J. Brown, S. L. Bowers, and J. A. Peoples

AFRL/RX

18 MARCH 2015
Interim Report

(STINFO COPY)

AIR FORCE RESEARCH LABORATORY
MATERIALS AND MANUFACTURING DIRECTORATE
WRIGHT-PATTERSON AIR FORCE BASE, OH 45433-7750
AIR FORCE MATERIEL COMMAND
UNITED STATES AIR FORCE

REPORT DOCUMENTATION PAGE

Form Approved
OMB No. 0704-0188

1. REPORT DATE *(DD-MM-YY)*	2. REPORT TYPE	3. DATES COVERED *(From - To)*
18 March 2015	Interim	17 January 2013 – 18 February 2015

4. TITLE AND SUBTITLE
COMPOSITIONAL CONTROL OF THE MIXED ANION ALLOYS IN GALLIUM-FREE InAs/InAsSb SUPERLATTICE MATERIALS FOR INFRARED SENSING (POSTPRINT)

5a. CONTRACT NUMBER
FA8650-07-D-5800-0006

5b. GRANT NUMBER

5c. PROGRAM ELEMENT NUMBER
62102F

6. AUTHOR(S)
1) H. J. Haugan, F. Szmulowicz, K. Mahalingam, G. J. Brown, S. L. Bowers, and J. A. Peoples - AFRL/RX

5d. PROJECT NUMBER
4348

5e. TASK NUMBER 0006

5f. WORK UNIT NUMBER
X0KY

7. PERFORMING ORGANIZATION NAME(S) AND ADDRESS(ES)
AFRL/RX
Wright-Patterson AFB, OH 45433-7750

8. PERFORMING ORGANIZATION REPORT NUMBER

9. SPONSORING/MONITORING AGENCY NAME(S) AND ADDRESS(ES)
Air Force Research Laboratory
Materials and Manufacturing Directorate
Wright-Patterson Air Force Base, OH 45433-7750
Air Force Materiel Command
United States Air Force

10. SPONSORING/MONITORING AGENCY ACRONYM(S)
AFRL/RXAN

11. SPONSORING/MONITORING AGENCY REPORT NUMBER(S)
AFRL-RX-WP-JA-2016-0251

12. DISTRIBUTION/AVAILABILITY STATEMENT
Distribution Statement A. Approved for public release: distribution unlimited.

13. SUPPLEMENTARY NOTES
PA Case Number: 88ABW-2015-1222; Clearance Date: 18 Mar 2015. This document contains color. Journal article published in SPIE Proceedings, Vol. 9609, 28 August 2015. © 2015 SPIE. The U.S. Government is joint author of the work and has the right to use, modify, reproduce, release, perform, display, or disclose the work.
The final publication is available at http://proceedings.spiedigitallibrary.org doi: 10.1117/12.2186188

14. ABSTRACT *(Maximum 200 words)*
Gallium (Ga)-free InAs/InAsSb superlattices (SLs) are being actively explored for infrared detector applications due to the long minority carrier lifetimes observed in this material system. However, compositional and dimensional changes through antimony (Sb) segregation during InAsSb growth can significantly alter the detector properties from the original design. At the same time, precise compositional control of this mixed-anion alloy system is the most challenging aspect of Ga-free SL growth. In this study, the authors establish epitaxial conditions that can minimize Sb surface segregation during growth in order to achieve high-quality InAs/InAsSb SL materials. A nominal SL structure of 77 Å InAs/35 Å InAs0.7Sb0.3 that is tailored for an approximately six-micron response at 150 K was used to optimize the epitaxial parameters. Since the growth of mixed-anion alloys is complicated by the potential reaction of As2 with Sb surfaces, the authors varied the deposition temperature (Tg) under a variety of Asx flux conditions in order to control the As2 surface reaction on a Sb surface.

15. SUBJECT TERMS
Gallium ; Indium arsenide ; Infrared detection ; Superlattices ; Antimony ; Infrared detectors ; Sensors

16. SECURITY CLASSIFICATION OF:			17. LIMITATION OF ABSTRACT:	18. NUMBER OF PAGES	19a. NAME OF RESPONSIBLE PERSON (Monitor)
a. REPORT	b. ABSTRACT	c. THIS PAGE			Gail Brown
Unclassified	Unclassified	Unclassified	SAR	11	19b. TELEPHONE NUMBER *(Include Area Code)* (937) 255-9854

Compositional control of the mixed anion alloys in gallium-free InAs/InAsSb superlattice materials for infrared sensing

H. J. Haugan, F. Szmulowicz, K. Mahalingam, G. J. Brown, S. L. Bowers, and J. A. Peoples

Air Force Research Laboratory, Wright-Patterson Air Force Base, Ohio 45433, USA

ABSTRACT

Gallium (Ga)-free InAs/InAsSb superlattices (SLs) are being actively explored for infrared detector applications due to the long minority carrier lifetimes observed in this material system. However, compositional and dimensional changes through antimony (Sb) segregation during InAsSb growth can significantly alter the detector properties from the original design. At the same time, precise compositional control of this mixed-anion alloy system is the most challenging aspect of Ga-free SL growth. In this study, the authors establish epitaxial conditions that can minimize Sb surface segregation during growth in order to achieve high-quality InAs/InAsSb SL materials. A nominal SL structure of 77 Å InAs/35 Å $InAs_{0.7}Sb_{0.3}$ that is tailored for an approximately six-micron response at 150 K was used to optimize the epitaxial parameters. Since the growth of mixed-anion alloys is complicated by the potential reaction of As_2 with Sb surfaces, the authors varied the deposition temperature (T_g) under a variety of As_x flux conditions in order to control the As_2 surface reaction on a Sb surface. Experimental results reveal that, with the increase of T_g from 395 to 440 °C, Sb-mole fraction x in $InAs_{1-x}Sb_x$ layers is reduced by 21 %, under high As flux condition and only by 14 %, under low As flux condition. Hence, the Sb incorporation efficiency is extremely sensitive to minor variations in epitaxial conditions. Since a change in the designed compositions and effective layer widths related to Sb segregation disrupts the strain balance and can significantly impact the long-wavelength threshold and carrier lifetime, further epitaxial studies are needed in order to advance the state-of-the-art of this material system.

1. INTRODUCTION

Following the proposal of type-II InAs/GaSb superlattice (SL) materials [1] for infrared application, there has been a great deal of research directed toward developing these materials for photodetector focal arrays. Owing to their relatively small SL periods, large absorption coefficient can be achieved due to enhanced electron-hole wave function overlaps [2-4]. More importantly, a large splitting between the heavy-hole and the light-hole bands in this SL reduces the hole-hole Auger recombination process [5], which improves device performance and operating temperature. One of the problems in this system, however, is the presence of Ga-mediated Shockley-Read-Hall (SRH) defects that are generated during epitaxy. The SRH defects shorten minority carrier lifetimes [6, 7] and degrade the detector performance [8, 9]. Recently, a similar type-II SL of InAs/InAsSb (noted herein as "Ga-free") has been proposed, and it has generated a great deal of interest due to the long SRH lifetimes observed in this material system. Carrier lifetimes up to ~10 microseconds have recently been demonstrated on materials with a properly band-gap engineered structure [10]. Such SL employs shorter periods in order to shift the SL band edges away from the SRH defect energy [10], which results in longer lifetimes. The epitaxial growth of Ga-free SL structures is relatively simple since only the antimony (Sb) composition needs to be varied across the layers. Initial growths of this material have succeeded in rapidly increasing carrier lifetimes from hundreds of nanoseconds to tens of microseconds. These results have encouraged several research groups to use Ga-free SLs for photodiode absorber layers. However, the epitaxial parameter space for the growth of this system still remains to be explored. Indeed, despite significant improvements in carrier lifetimes, most measured detectivities (D*) of Ga-free SL photodiodes [11] are still lower than those for InAs/GaSb (noted herein as "Ga-containing") SL diodes [9]. In particular, D* depends not only on SRH lifetime but also on other recombination sources (such as Auger and radiative) as well as on the collection quantum efficiency, the background carrier concentration, the vertical minority carrier mobility, and other potential materials-related issues. These issues have prompted a reexamination of the intrinsic electronic structure of the SL [9, 11] and of the epitaxial growth processes in

Infrared Sensors, Devices, and Applications V, edited by Paul D. LeVan, Ashok K. Sood, Priyalal Wijewarnasuriya, Arvind I. D'Souza, Proc. of SPIE Vol. 9609, 960906

order to continue to advance the state of this material system for infrared detector applications. One major issue in the Ga-free epitaxy is significant Sb compositional grading at both the Sb-on-As and As-on-Sb interfaces [13, 14]. The lack of abrupt interfaces and compositional uniformity control in each layer results in as-grown SLs with optical and electrical properties, which are very different from the intended SL design. These unintended compositional gradients also impact the strain balance of the SL. Whereas the original design is lattice matched to the GaSb substrate, a change in the designed compositions and effective layer widths disrupts the strain balance of the two layers that is needed to achieve lattice matching. Therefore, detailed epitaxial process studies are needed to advance the state-of-the-art of this material system.

In this report, our goal is to establish the molecular beam epitaxy (MBE) growth processes that can produce high-quality, Ga-free SL materials tailored for a specific infrared band gap in the mid-infrared range. To accomplish this goal, a series of epitaxial optimization studies was performed using a nominal SL structure of 77 Å InAs/35 Å $InAs_{0.7}Sb_{0.3}$ designed for an approximately six-micron response at 150 K [15]. This SL covers the 3-5 µm wavelength range and suppresses electron-electron Auger recombination in an n-type SL. Since compositional control of the mixed anion alloys is critical for achieving an accurate structure for the photodetector application, we discuss how to optimize Sb incorporation during InAsSb layer epitaxy in order to grow a strain-balanced, Ga-free SL structure.

2. THEORETICAL PROSPECTIVE

The intrinsic electronic properties of the Ga-free InAs/InAsSb and the Ga-containing InAs/GaSb SLs were investigated in order to compare the two mid-infrared SL designs. The band structures, wave functions, and oscillator strengths were calculated using our 8 x 8 envelope-approximation model described in reference [16], and the linear absorption coefficient was found using the Gilat-Raubenheimer k-space integration technique with a very fine subdivision of the Brillouin zone into cubes. Figure 1 shows the calculated band structures for the two materials in the near band gap region.

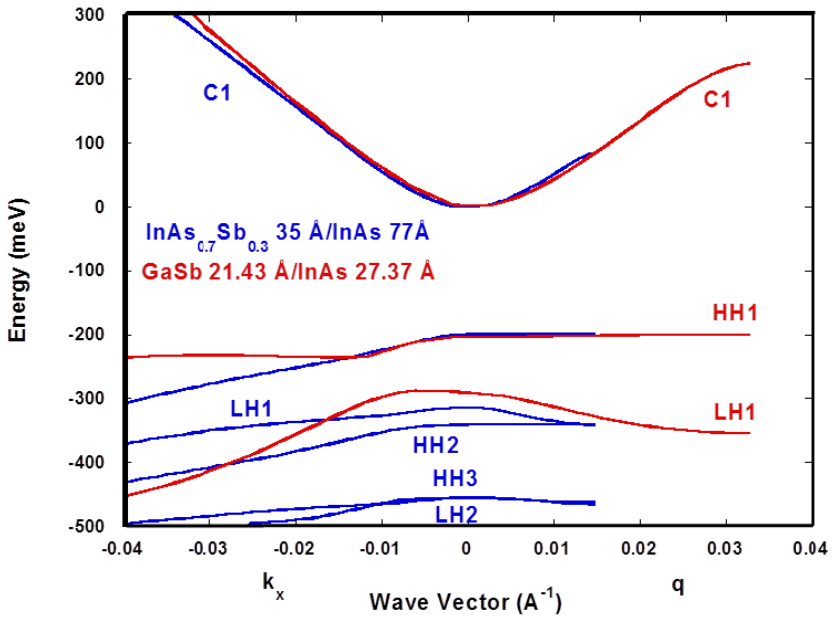

Figure 1. The calculated band structure for the Ga-free InAs/InAsSb and the Ga-containing InAs/GaSb superlattices with mid-infrared gap at 5 K.

Because of its longer period, the Brillouin zone for the Ga-free SL is shorter. The band gaps of the two SLs are the same. The conduction bands are similar since the electron mass derives mainly from the bulk electron mass of InAs, a material that is common to both SLs. However, there are large differences in the valence bands of the two materials. First, owing to its wider InAsSb layer width and a larger perpendicular hole mass, the Ga-free SL has a greater number of valence bands in the immediate vicinity of the band gap. Such a concentration of bands is not beneficial to Auger process suppression and to the resulting Auger lifetimes. The masses for the heavy-hole (HH) bands in the growth direction for the two materials are effectively infinite, indicating that heavy holes are largely confined in the respective InAsSb and GaSb layers. The light-hole (LH) mass for the Ga-containing SL is lighter and the HH mass heavier in the in-plane direction than the corresponding masses for the Ga-free SL as a result of an avoided-crossing that is partly due to the interface terms in the Hamiltonian for the Ga-containing SL.

Figure 2 shows the calculated linear absorption coefficients at 5 K for in-plane polarized light. The two graphs have the same shape near the onset of absorption and have a similar kink at higher energies related to the onset of the LH1-to-C1 (first conduction band) absorption. The clear difference is in the magnitude of the absorption, with the absorption for the Ga-containing SL being stronger and rising faster than is the case for the Ga-free SL. The difference is due to the larger oscillator strength for the Ga-containing SL, which is connected with the smaller InAs layer width and the overall narrower SL width. Overall, the Ga-containing SL has the advantage of higher absorption, a sharper absorption onset, and longer Auger lifetimes.

Antimony segregation for the Ga-free SL leads to the presence of Sb in the InAs layers and in diffused, ternary $InAs_ySb_{1-y}$ interfaces. The resulting valence and conduction band potential profiles are above those for InAs. Consequently, the conduction band-well bottom lifts up, which raises the C1; also, the potential well height for holes decreases, which results in a shallower valence band well, a raised HH1, and additional valence bands drawn into the well. The effect is greater on C1, so the band gap will increase; also, owing to the greater density of valence bands, the minority carrier Auger lifetime in p-type SLs will decrease. Antimony diffusion into InAs will also narrow the effective InAsSb and InAs layers widths, which will lead to energy shifts due to size-quantization effects. Theory predicts an about 15 % narrowing of the band gap between 5 and 150 K. Antimony inter-diffusion will affect the wave functions, the oscillator strengths, and the resulting near-band-gap absorption, including the long-wavelength threshold. Since interface-roughness scattering is a leading mobility-limiting mechanism in SLs, the altered interface geometry due to diffusion should also have a profound effect on carrier mobilities.

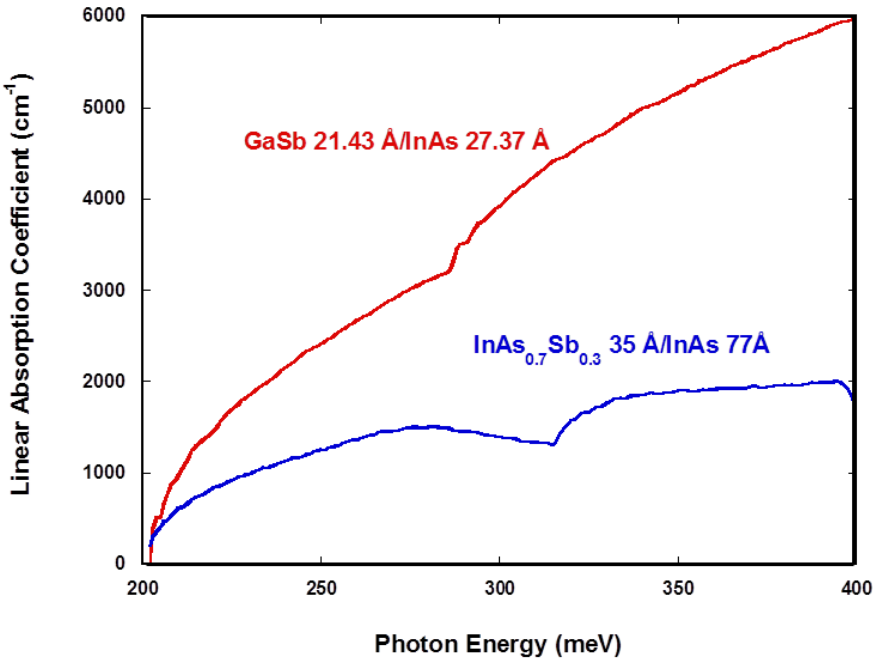

Figure 2. The calculated absorption coefficients for the Ga-free InAs/InAsSb and the Ga-containing InAs/GaSb superlattices at T = 5 K.

3. GALLIM-FREE SUPERLATTICE GROWTHS

In order to investigate how the epitaxial growth conditions impact the Sb incorporation for the selected 77 Å InAs/35 Å $InAs_{0.7}Sb_{0.3}$ SL design, SL samples were grown on GaSb (100) substrates by MBE. The 45 repeated SL periods (0.5 µm thick) were deposited on the undoped GaSb buffer layer (0.5 µm thick) and capped with a 100 Å GaSb layer. To grow the intended structure, a V/III beam equivalent pressure (BEP) ratio of 3 for the InAs layer growth, and a Sb/As BEP ratio of ~0.4 for the InAsSb layer growth, were used. Since the composition of the individual layers is extremely sensitive to the incident anion flux and its surface reaction at the growth surface, the SL layers were deposited at growth temperatures (T_g) ranging from 395 to 440 °C in order to optimize Sb incorporation during epitaxy, and the growth rate between 1.0 and 0.5 Å/s was used for InAs (R_{InAs}) layer. The Sb cracking zone temperature was fixed at 950 °C, however the As cracking zone temperature was varied from 950 to 750 °C in order to investigate As_x surface reaction during InAsSb layer growth. Triple axis (004) high-resolution x-ray (HRXRD) was collected for all grown SL samples to extract the SL period and residual strain; commercial X'pert epitaxy simulation software was used to estimate individual layer thicknesses and their compositions. Figure 3 shows the X-ray diffraction profile of a typical, strain-balanced, Ga-free SL structure, demonstrating the excellent crystalline quality that can be achieved by using the growth conditions described above. Figure 4 shows a transmission electron microscopy image of a Ga-free SL structure grown for the present study. The image was obtained using the high-angle annular dark-field imaging technique, wherein the InAs and InAsSb layers exhibit dark and bright contrast, respectively. The average SL period was measured to be 114 ± 1 Å, with an average layer thickness of 76 ± 2 Å for InAs and 38 ± 3 Å for InAsSb (with accuracy limited by uncertainties in input parameters), which is close to the intended SL structure.

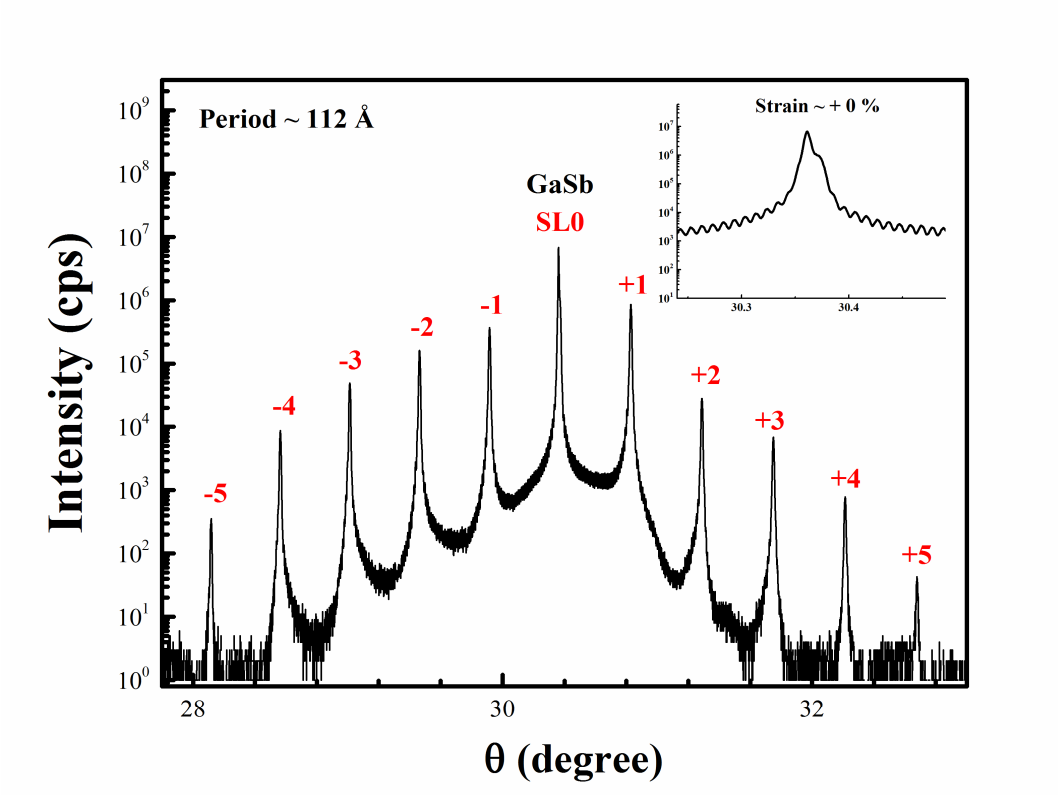

Figure 3. X-ray diffraction patterns of a strain-balanced, Ga-free superlattice structure of a 77 Å InAs/35 Å $InAs_{0.7}Sb_{0.3}$.

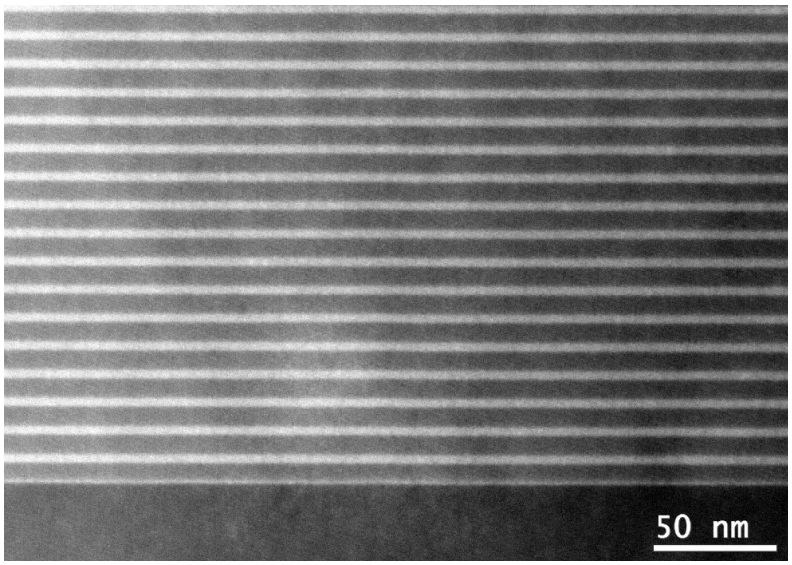

Figure 4. A High-angle annular dark field transmission electron microscopy image for the Ga-free superlattice structure of a 77 Å InAs/35 Å $InAs_{0.7}Sb_{0.3}$.

4. RESULTS AND DISCUSSIONS

Since the band gap of the SL and related optical properties are very sensitive to the layer fluctuations and compositional variations, the most challenging aspect of Ga-free SL growth is the precise growth control of the individual layers and their alloy compositions, which is non-trivial. Since the growth of mixed anion alloys is complicated by the potential reaction of As_2 with Sb surfaces, we varied the deposition temperature in order to control the As_2 surface reaction on a Sb surface under two different As_x flux conditions. Since As_2 is much more volatile than Sb_2, the competition between As_2 and Sb_2 for reactive sites on the growth surface is preferentially weighted toward As_2, and generally uncracked As_4 species can suppress surface reaction more than cracked As_2 ones [17], we investigate the As_4 effect on the efficiency of Sb_2 incorporation by manipulating T_g and As cracking zone temperatures, no systematic study was done to determine the As_2/As_4 ratio as a function of cracking zone temperature for our Mark V 500 cc Arsenic Valved Cracker. A first series of five SL samples with T_g set at 395, 405, 415, 430, and 440 °C was grown back to back under the following growth condition, designated as "high As flux condition": V/III BEP ratio of 3 for InAs layer growth, R_{InAs} of ~1 Å/s, Sb/As BEP ratio of ~0.4, and cracking zone temperature of 950 °C for both Sb and As. Figure 5 shows the HRXRD profiles of the (400) reflection for the SL sample series. The profiles show a systematic change in the separation between the substrate and SL peak, indicating that the Sb composition x in $InAs_{1-x}Sb_x$ layer (and the corresponding tensile strain) gradually decreases (increases) with increasing T_g (see Figure 5 insert). Table I provides a summary of the structural results measured by HRXRD. It is important to realize that while the SL periods and SL net strain could be determined accurately by HRXRD, the individual layer thicknesses (d) and x could only be estimated using the calibrated growth rate and the simulations. Based on the simulated results, the sample grown at the lowest T_g of 395 °C had the highest x that is close to the intended x of 0.3, and the Sb incorporation was suppressed by 21 % as T_g increased from 395 to 440 °C, which proves that the incorporation efficiency of Sb is sensitive to the deposition temperature. This finding differs from the results observed in such mixed-cation alloy system as InAs/InGaSb SLs, where the SL net strain remains constant regardless of T_g [18-22].

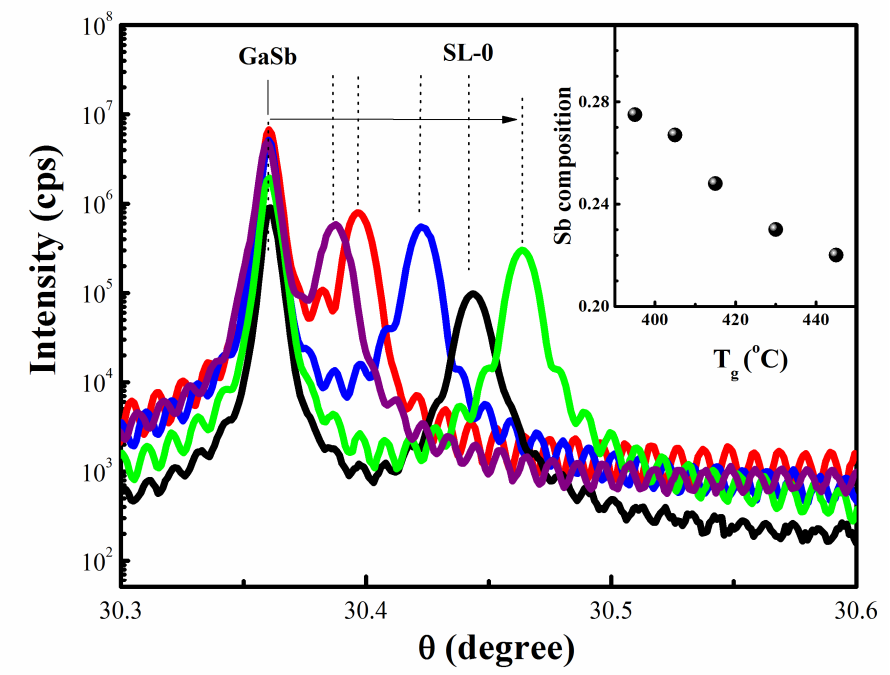

Figure 5. X-ray diffraction profiles of the (400) reflection, showing the GaSb substrate and superlattice (SL) peaks for Ga-free SL samples deposited at various temperatures (T_g) under high As flux condition. The insert shows the Sb composition as a function of T_g.

Table I. Structural parameters of $InAs/InAs_{1-x}Sb_x$ superlattices (SLs). Growth temperature, SL period, layer thickness, and Sb composition are noted by T_g, P, d, and x, respectively. Commercial X'pert epitaxy simulation software was used to estimate the d and x. The arsenic cracking zone temperature was set at 950 °C.

Sample	$T_g \pm 3$ (°C)	$P \pm 0.5$ (Å)	Strain (%)	$d_{InAs} \pm 0.5$ (Å)	$d_{InAsSb} \pm 0.5$ (Å)	$x \pm 0.01$
SL1	395	109	-0.08	76	33	0.28
SL2	405	108	-0.11	75	33	0.27
SL3	415	109	-0.18	76	33	0.25
SL4	430	109	-0.24	76	33	0.23
SL5	440	109	-0.30	76	33	0.22

A second series of four SL samples with T_g set at 395, 410, 420, 430, and 440 °C was grown back to back under the following growth conditions, designated as "low As flux condition": V/III BEP ratio of 3 for InAs layer growth, R_{InAs} of ~0.5 Å/s, Sb/As BEP ratio of ~0.4, and cracking zone temperature of 950 °C for Sb and 900 °C for As. Figure 6 shows the X-ray diffraction profiles for the SL sample series. The X-ray profiles show a systematic change in the separation between the substrate and the SL peak, indicating the Sb composition x in the $InAs_{1-x}Sb_x$ layer (and the corresponding tensile strain) systematically decreases (increases) with increasing T_g (see Figure 6 insert). The sample grown at the lowest T_g also produced the highest x that is close to the intended x of 0.3, and its Sb incorporation was suppressed only by 14 % as T_g increased from 395 to 440 °C. It is apparent that the incorporation efficiency of Sb is extremely sensitive to minor variations in epitaxial parameters. Table II summarizes the structural results for second sample series.

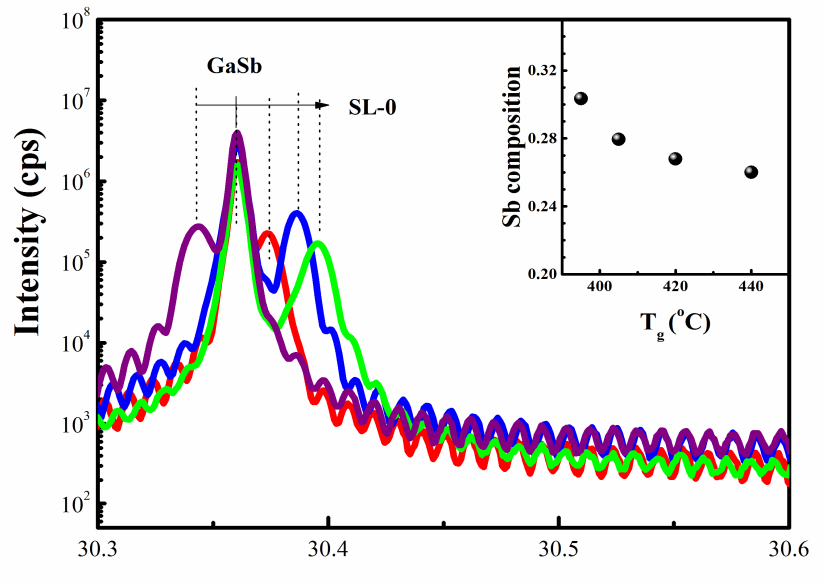

Figure 6. X-ray diffraction profiles of the (400) reflection, showing the GaSb substrate and superlattice (SL) peaks for Ga-free SL samples deposited at various temperatures (T_g) under low As flux condition. The insert shows the Sb composition as a function of T_g.

Table II. Structural parameters of $InAs/InAs_{1-x}Sb_x$ superlattices (SLs). Growth temperature, SL period, layer thickness, and Sb composition are noted by T_g, P, d, and x, respectively. Commercial X'pert epitaxy simulation software was used to estimate the d and x. Arsenic cracking zone temperature was set at 900 °C.

Sample	$T_g \pm 3$ (^{o}C)	$P \pm 0.5$ (Å)	Strain (%)	$d_{InAs} \pm 0.5$ (Å)	$d_{InAsSb} \pm 0.5$ (Å)	$x \pm 0.01$
SL6	395	109	+0.05	76	33	0.30
SL7	410	110	-0.04	76	34	0.28
SL8	420	111	-0.07	76	35	0.27
SL9	440	112	-0.10	76	36	0.26

5. CONCLUSIONS

In conclusion, we investigated the effect of growth temperature (T_g) on Sb-mole fraction x in $InAs_{1-x}Sb_x$ layers, using a nominal 77 Å InAs/35 Å $InAs_{0.7}Sb_{0.3}$ SL structure that is tailored for an approximately six-micron response at 150 K. Experimental results show that the SL samples grown at the lowest investigated T_g of 395 °C produce the highest Sb content (x) of ~0.3 in general. However, Sb composition decreased by 21 % under the high As flux condition and by only 14 % under the low As flux condition, when T_g increased from 395 to 440 °C, which demonstrates the sensitivity of Sb incorporation to epitaxial conditions. According to our theoretical calculations, absorption for the Ga-containing SLs is stronger and rises faster than for the Ga-free SLs due to the differences in the SL layer widths. Theory predicts that Ga-containing SLs generally have the advantage of higher absorption, sharper absorption onset, and longer Auger lifetimes than Ga-free SLs. Antimony segregation will affect the band structure, the wave functions, and the oscillator strengths, hence the resulting near-band-gap absorption, the long-wavelength threshold, carrier lifetime, and mobility. Therefore, there is a need for continued epitaxial study in order to advance the state-of-the-art of the Ga-free material system.

ACKNOWLEDGMENTS

The work of H. J. Haugan and F. Szmulowicz was performed under Air Force contract number FA8650-11-D-5800 and FA8650-11-D-5401, respectively. One of Authors (H. J. Haugan) would like to thank Professor C. H. Grein for helpful discussions about gallium-free superlattice design used in this study. Haugan designed the epitaxy study series, did superlattice (SL) growths and X-ray simulations, and wrote the main manuscript. Szmulowicz did theoretical calculation of Ga-containing and Ga-free SL designs used in here. Mahalingam did TEM and its analysis. Brown did technical editing of the manuscript. Bowers and Peoples provided technical assistance with the MBE system and X-ray measurements, and sample preparation for the TEM measurements, respectively.

REFERENCES

[1] D. L. Smith, C. Mailhiot, J. Appl. Phys. **62**, 2545 (1987).
[2] H. J. Haugan, F. Szmulowicz, G. J. Brown, K. Mahalingam, J. Appl. Phys. **96**, 2580 (2004).
[3] H. J. Haugan, F. Szmulowicz, G. J. Brown, B. Ullrich, S. R Munshi, L. Grazulis, K. Mahalingam, S. T. Fenstermaker, Physica E **32**, 289 (2006).
[4] H. J. Haugan, K. Mahalingam, G. J. Brown, W. C. Mitchel, B. Ullrich, L. Grazulis, S. Elhamri, J. C. Wickett, D. W. Stokes, J. Appl. Phys. **100**, 123110 (2006).
[5] C. H. Grein, W. H. Lau, T. L. Harbert, M. E. Flatté, Proc. SPIE. **4795**, 39 (2002).
[6] D. Donetsky, S. P. Svensson, L. E. Vorobjev, G. Blenky, G. Blenky, Appl. Phys. Lett. **95**, 212104 (2009).
[7] S. P. Svensson, D. Donetsky, D. Wang, H. Hier, F. J. Crowne, G. Blenky, J. Cryst. Growth **334**, 103 (2011).
[8] E. Plis, S. J. Lee, Z. Zhu, A. Amtout, S. Krishna, Quantum Electron. **12**, 1269 (2006).
[9] C. Downs and T. E. Vandervelde, Sensor **13**, 5054 (2013).
[10] Y. Aytac, B. V. Olson, J. K. Kim, E. A. Shaner, S. D. Hawkins, J. F. Klem, M. E. Flatté, T. F. Boggess, Appl. Phys. Lett. **105**, 022107 (2014).
[11] H. S. Kim, O. O. Cellek, Zhi-Yuan Lin, Zhao-Yu He, Xin-Hao Zhao, Shi Liu, H. Li, Y.-H. Zhang, Appl. Phys. Lett. **101**, 161114 (2012).
[12] B. V. Olson, E. A. Shaner, J. K. Kim, J. F. Klem, S. D. Hawkins, L. M. Murray, J. P. Prineas, M. E. Flatté, T. F. Boggess, Appl. Phys. Lett. **101**, 092109 (2012).
[13] M. R. Woods, K. Kanedy, F. Lopez, M. Weimer, J. F. Klem, S. D. Hawkins, E. A. Shaner, J. K. Kim, J. Cryst. Growth **425**, 110 (2015).
[14] K. Mahalingam, E. H. Steenbergen, G. J. Brown, and Y.-H. Zhang, Appl. Phys. Lett. **103**, 061908 (2013).
[15] C. H. Grein at the II-VI Workshop (2013) and via personal communication.
[16] F. Szmulowicz, H. Haugan, G. J. Brown, Phys. Rev. B **69**, 155321 (2004).
[17] B. Z. Nosho, B. R. Bennett, and L. J. Whitman, and M. Goldenberg, J. Vac. Sci, Technol. B **19**, 1626 (2001).

[18] H. J. Haugan, G. J. Brown, S. Elhamri, W. C. Mitchel, K. Mahalingam, M. Kim, G. T. Noe, N. E. Ogden, and J. Kono, Appl. Phys. Lett. **101,** 171105 (2012).
[19] H. J. Haugan, G. J. Brown, M. Kim, K. Mahalingam**,** S. Elhamri, W. C. Mitchel, and L. Grazulis**,** Proc. SPIE. **8704**, 39 (2013).
[20] Heather J. Haugan, Gail J. Brown, Krishnamurthy Mahalingam, Larry Grazulis, Gary T. Noe, Nathan E. Ogden, and Junichiro Kono, J. Vac. Sci. Technol. **B 32**, 2C109 (2014)
[21] H. J. Haugan, G. J. Brown, K. Mahalingam, and L. Grazulis, Infrared Phys. Technol. **70**, 99 (2015).
[22] H. J. Haugan, G. J. Brown, S. Elhamri, and L. Grazulis, J. Cryst. Growth **425**, 25 (2015).